Synthesis and Characterization of Novel Antibacterial PDDA/Honey Nanofiber Against Gram-Positive and Gram-Negative Bacteria

Ghazaleh Chiari Fard [1,2], Laleh Maleknia [1,3], Masoud Giahi [1,4], Arash Almasian [1], Mohammad Shabani [2], S. Ahmad Dehdast [1,2*]

[1] Nanotechnology Research Center, Islamic Azad University- Tehran South Branch, Tehran, Iran

[2] Department of Biochemistry, School of Medicine, Iran University of Medical Sciences, Tehran, Iran

[3] Department of Biomedical Engineering, Islamic Azad University, South Tehran Branch, Tehran Iran

[4] Department of Chemistry, Lahijan Branch, Islamic Azad University, Lahijan, Iran

ARTICLE INFO

ABSTRACT

Nanomaterials are increasingly used to the targeting of gram-positive and gram-negative bacteria as an alternative to antibiotics. Bacterial infections are a major cause of chronic infections and mortality. People requirement for new materials for pathogenic bacteria treatment. It seems that nanomaterial-based strategies can be resolving this problem. In this research, improved antibacterial nanofibrous material using the synthesis of novel blend nanofibers by electrospinning method against gram-positive and gram-negative bacteria. First, Honey as a natural, biocompatible and antimicrobial compound (with different percentages) was added to the PDDA solution and the influence of processing parameters on the morphology of the electrospun blend nanofibers were investigated. The results showed that a bead-free morphology of nanofibers with uniform diameter achieved at the concentration ratio of 40/60% (PDDA/honey), the flow rate of 0.8 mL/h and the high voltage of 17kV. The sample with optimum morphology was cross-linked by glutaraldehyde at different crosslinking times. Evaluation of the water absorption property of nanofibers showed the absorption capacity of 4.9 g/g. Then, the in-vitro antibacterial activity of nanofiber investigated against gram-positive and gram-negative strains, Staphylococcus aureus (S. aureus) and Escherichia coli (E. coli). Afterward, novel nanofiber antibacterial activity studied against pathogenic Pseudomonas aeruginosa (P. aeruginosa). The MIC values indicated that the ratio of 40/60% PDDA/honey nanofiber induced about 99.9% bacterial death for both strains. Moreover, the novel PDDA/honey nanofibers showed suitable antibacterial activity (98.89 %) against pathogenic Pseudomonas aeruginosa. Moreover, the results showed a large reduction of bacterial numbers and evidently presented novel nanofibers as new antimicrobial agents.

INTRODUCTION

The treatment of bacterial infections has been dramatically compromised by the persistent emergence of gram-positive and gram-negative antibiotic resistant strains (1,2). The Gram-negative bacterium Pseudomonas aeruginosa is an opportunistic pathogen that normally inhabits the soil and surfaces in aqueous environments such as water and soil ecosystems and infective to plants, animals and humans (3-5). Pseudomonas aeruginosa is considered the most medically important among the genus Pseudomonas that frequently causes hospital-acquired and opportunistically infections for example pneumonia, urinary tract infections and wound

* Corresponding Author Email: *arashdehdast@gmail.com*

infections (6,7). Infections caused by P. aeruginosa are often severe and life threatening and are difficult to treat because of the limited susceptibility to antimicrobial agents. (8). Pseudomonas aeruginosa is a notoriously difficult organism to control with antibiotics or disinfectants. (9). On the other hand, Nanoantibiotics have recently developed as a hopeful technology to improve outcomes of infections. moreover, attention has been focused on novel attractive nano-based materials with antibacterial activity. (10,11). In the last few years, one-dimensional nanomaterials such as nanofibers, nanowires and nanorods have been attracting a great interest of researchers due to their unique optical, thermal, electrical, magnetic, and mechanical properties and they have been used in many applications such as catalysis, energy storage, nanoreactors, sensors, drug delivery and biomedical engineering [12,13]. The main advantage of one-dimensional structures is their high surface area, which provides many special properties and functionalities [14].

Electrospinning technique is a simple, convenient, low cost and versatile method which has been used to produce one-dimensional nanostructure materials [15]. Most soluble polymers with appropriate molecular weight can be electrospun. Polymeric nanofibers have been used in many applications including filters, reinforcing agents, biomedical materials, tissue engineering, catalysis, sensing, fabrication of composite materials, supercapacitors, fiber templates to prepare nanotubes and wound dressing [16-18]. Also, this technique has the ability to produce a three-dimensional nanofibrous membrane with a large surface area [19].

Poly (diallyldimethylammonium chloride) (PDDA) is a linear cationic polyelectrolyte which is widely used in industrial applications such as flocculants, dewatering agents, emulsifiers, papermaking, mining and petrol industry [20]. Also, it is used as a model for studies in different areas of polyelectrolyte research and functionalizing nanomaterials [21]. The functionalized graphene nanosheets with PDDA were synthesized and used to combine with room temperature ionic liquid (RTIL) [22]. Formation of unique micro- and nanostructures from the combination of the anionic surfactant sodium dodecyl sulfate (SDS) with cationic PDDA polyelectrolyte was evaluated [23]. In another research, PDDA and Sodium

Silicate Multilayers are coated on silica-sphere to prepare a superhydrophobic surface [24].

On the other hand, the polyelectrolyte PDDA has been considered as a safe compound for human health. Also, it has a biocompatible, biodegradable and nontoxic nature. This homopolymer bears permanently charged quaternary ammonium groups in its cyclic unities which enable it to be classified as antimicrobial agents [25]. Cationic bilayer fragment/ carboxymethylcellulose (CMC)/ PDDA nanoparticle with high antibacterial property is synthesized by researchers [26]. Also, the antimicrobial activity of PDDA/ poly (methylmethacrylate) nanoparticles is investigated [27]. The cationic bilayer fragments/amphotericin B/carboxymethyl cellulose/ PDDA nanoparticles with the releasing ability of amphotericin B are prepared [28].

Moreover, Honey is a natural high nutritional and prophylactic viscous food which is generally composed of water, glucose, sucrose, fructose, and many other substances. Honey is shown medicinal properties and it has been used in wound care due to its antimicrobial property [29]. Also, the fabrication of the electrospun honey-based fibrous matrices could be possible. In this regard, the poly (vinyl alcohol) (PVA)/honey electrospun fibers with a uniform and bead-free morphology are prepared [30]. Also, the polyethylene terephthalate (PET)/ honey/chitosan nanofibers aiming to produce a wound dressing are produced [31]. However, a literature review showed that there is no study on preparation of PDDA or PDDA/ honey nanofibers. In this research, the ability of the PDDA nanofibers producing with two molecular weights and antibacterial activity of novel antibiotic free antibacterial PDDA/honey nanofiber was investigated. The amount of honey in the spinning solution and the electrospinning parameters were optimized aiming to produce a uniform and bead-free morphology. Finally, the obtained nanofibers were crosslinked by glutaraldehyde to decrease the solubility and improve the water absorption property. Antibacterial results showed that the PDDA/honey nanofibers have been high antibacterial activity against gram-positive and gram-negative bacteria. Moreover, investigation of antibacterial activity of antibiotic free nanofiber against Pseudomonas aeruginosa (P. aeruginosa) demonstrated the novel PDDA/honey nanofiber is suitable agent for the treatment of pathogenic P. aeruginosa infection.

EXPERIMENTAL

Materials

Poly (diallyldimethylammonium chloride) (PDDA) with the medium molecular weight (M_w=200,000-350,000), 20 *wt%* in H_2O and high molecular weight (M_w=450,000), 40 *wt%* in H_2O were purchased from Sigma Aldrich (Germany). Raw Persian Honey in name of Thyme was purchased from a local producer (Polour, Iran). Glutaraldehyde (GA) (50% in water) was as received from Merck (Germany).

Preparation of nanofibers

The PDDA solution was used as received without any change in its concentration. The produce ability of PDDA nanofibers was investigated at different conditions including wide ranges of high voltage (14-23 *kV*) and feeding rate (0.35-1*mL/h*). In order to produce the PDDA/honey nanofibers, different spinning solutions was prepared by adding the various amount of honey (30-70%*w/w*, respect to the PDDA) to the PDDA solution. Then, 1 *m*L ethanol was added to the solutions (the volume of mixed solution was 5 *mL*) under stirring at room temperature for 1*h*. The prepared solutions were then electrospun under a wide range of high voltage (14-23 *kV*) when the distance between tip of needle and collector was 16*cm*. The electrospinning apparatus was from Fanavaran nano-meghyas Co. (Iran) and nanofibers were collected onto aluminum (Al) sheet. The feeding rate of the polymer solution was changed in range of 0.35-1 *mL/h*.

Crosslinking of nanofibers

The nanofiber mats (15 *cm*×15 *cm*) were attached to polyethylene frames and placed into a sealed chamber saturated with the vapor of 40 *mL* of GA solution. The nanofibers were exposed to GA vapor for different times (2, 3, 4 and 5) and then placed in a vacuum oven at 70 *°C* for 12 *h* to remove residual glutaraldehyde.

Characterization

The surface morphology of nanofibers was characterized by Scanning Electron Microscope (SEM, LEO1455VP, ENGLAND). The FTIR spectra of nanofibers were examined by the FTIR spectroscopy (ThermoNicolet NEXUS 870 FTIR from Nicolet Instrument Corp., USA).

The antibacterial activity of nanofibers against Escherichia coli (ATCC 25922) a Gram-negative bacteria and S. aureus (ATCC 25923) a Gram-positive bacterium was measured by using the viable cell counting method. 100 *µL* E. coli and S. aureus were cultivated in 100 *mL* of a nutrient broth solution individually. Then, 1 *mL* of the bacteria/nutrient solution was added to 9 *mL* of sterilized nutrient broth solution (0.8%). Bacteria concentration of $5×10^5$ *CFU/mL* was selected for the test. The weight and size of samples were 100 *mg* as disks of 2.8 *cm* diameter. The antibacterial test was performed by putting the nanofibers into 10 *mL* of the bacteria/nutrient solution. After the exposure of the bacteria to the nanofibers, the bacterial solution (100 *µL*) was taken out and quickly spread on a plate containing nutrient agar. Plates containing bacteria were incubated at 37 *°C* for 24 *h*, and then the numbers of the surviving colonies were counted.

Water absorbency measurement was performed via gravimetric analysis. 0.10 *g* of nanofibers was immersed in 50 *mL* of distilled water at room temperature (25 *°C*) for 120 *min* and pH=7.4. Then, the nanofibers were separated and weighed. The water absorbency (Q; *g.g⁻¹*) was calculated as follows.

$$Q = \frac{m_a - m_b}{m_b} \tag{1}$$

where m_b (g) and m_a (g) are the weights of the samples in the dry state and the swollen state at a certain time, respectively [32].

The solubility of nanofibers was investigated by immersing the nanofibers in a batch containing distilled water for 120 *min* at 25*°C* and pH=7.4. After that, the nanofibers were separated and dried at 60*°C* for 6*h*. They were weighed and the solubility was calculated using the following equation.

$$Solubility\,(\%) = \frac{m_X - m_y}{m_y} \times 100 \tag{2}$$

where m_x and m_y are the weight of nanofibers before and after the immersing in distilled water, respectively.

RESULTS AND DISCUSSION

In order to control the fiber characteristics, the electrospinning parameters can be adjusted. Viscosity, molecular weight of the polymer, applied voltage, charge density and distance from needle to collector are of important parameters affecting
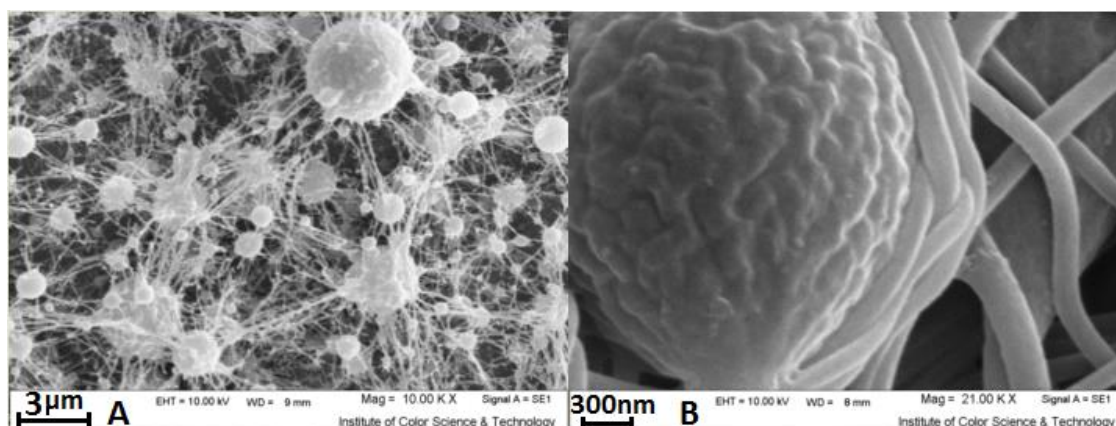
Fig. 1. The SEM images of A and B) PDDA nanofibers at different magnifications

directly on the nanofiber morphology [31].

In this study two molecular weights of PDDA polymer were used to produce nanofibers. The nanofibers could not be obtained with lower molecular weight of PDDA polymer. Fig. 1 showed the SEM images of PDDA nanofibers prepared by the polymer with high molecular weight at different magnifications. A wide range of high voltage (14-23 kV) was applied to the polymer droplet to produce fibrous structure. As can be seen, many defects such as bead and droplets existed in the nanofiber morphology. Also, there were a lot of unspun droplets during the process which was resulted from the influence of the gravitational force [33]. However, the reproducibility of spinning procedure was not feasible and the electrospinning conditions including flow rate and voltage were varied for each test. Reproducibility and stability are the important factors of the electrospinning process [34]. The formation of droplets among the nanofibers can be due to the capillary breakup of the spinning jet by surface tension. In this case, the distance of polymer chains in the solvent were relatively far and the effective entanglement could not be occurred.

In order to enhance the spinning conditions and obtain a uniform morphology, honey with different concentrations (30, 40, 50, 60 and 70%w/w respect to PDDA concentration) was added to the PDDA solution. Nanofibers with the concentration ratio of 70/30, 60/40 and 30/70%w/w (PDDA/honey) were not obtained. At low concentration of honey (30 and 40%w/w), the viscosity of solution was low and a long continuous liquid jet was not formed. On the other hand, raising the honey concentration

to 70%w/w caused to a significant increase in the viscosity value of spinning solution. Higher viscosity values result to higher entanglement of the polymer chains [35]. Fig. 2 showed the changes of the viscosity as a function of the shear rate for various solutions at 25°C. It was clear that the shear thinning effect occurred for the PDDA solution (the viscosity decreases with raising the shear rate). In this case, at low shear rates, the polymer chains are not aligned with the direction of flow. This caused to appearance of a relatively high viscosity value. With increasing the shear rates, the number of aligned polymeric chains to the direction of flow increased resulted to a lower viscosity value.

Honey with different origins showed various rheological behaviors. Most of the honeys are reported to have Newtonian fluid like characteristics, whereas, some honey showed non-Newtonian fluids properties [36]. Some others also exhibited a thixotropic behavior [37]. The thyme Persian honey, which was used in this study, showed a Newtonian fluid like characteristics. The apparent viscosity remained nearly constant with increasing shear rates. Such a result is reported by other researchers [38]. However, the PDDA solution with concentration ratio of 30/70, 40/60 and 50/50 showed a Newtonian fluid like behavior which can be due to the high concentrations of honey in the mixed solution. With increasing the PDDA concentration the changes in the viscosity values increased. For the solutions with the PDDA concentration of 60 and 70%w/w, the viscosity decreased with raising the shear rate (shear thinning effect). The viscosity value for the PDDA, honey, and the 70/30, 60/40, 50/50, 40/60, 30/70
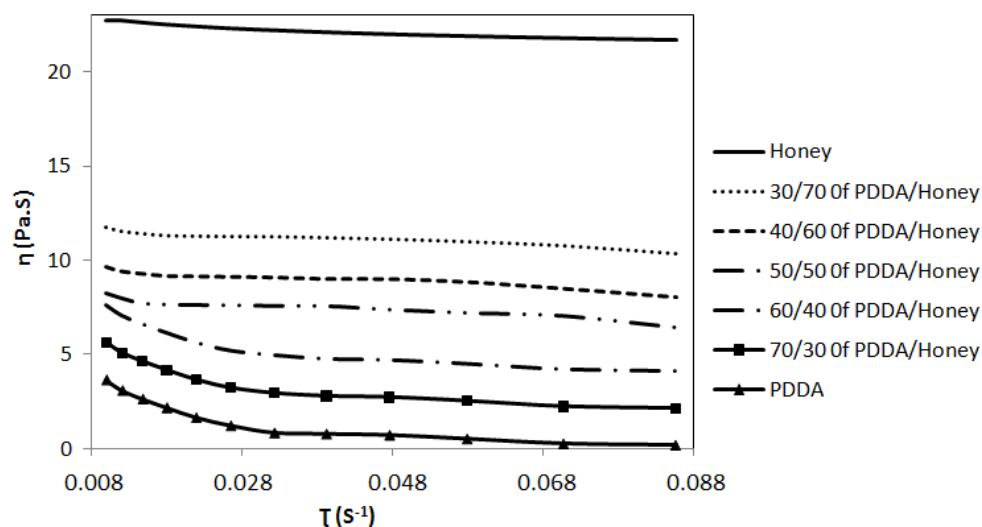
Fig. 2. the changes of the viscosity as a function of the shear rate for various solutions at 25°C.
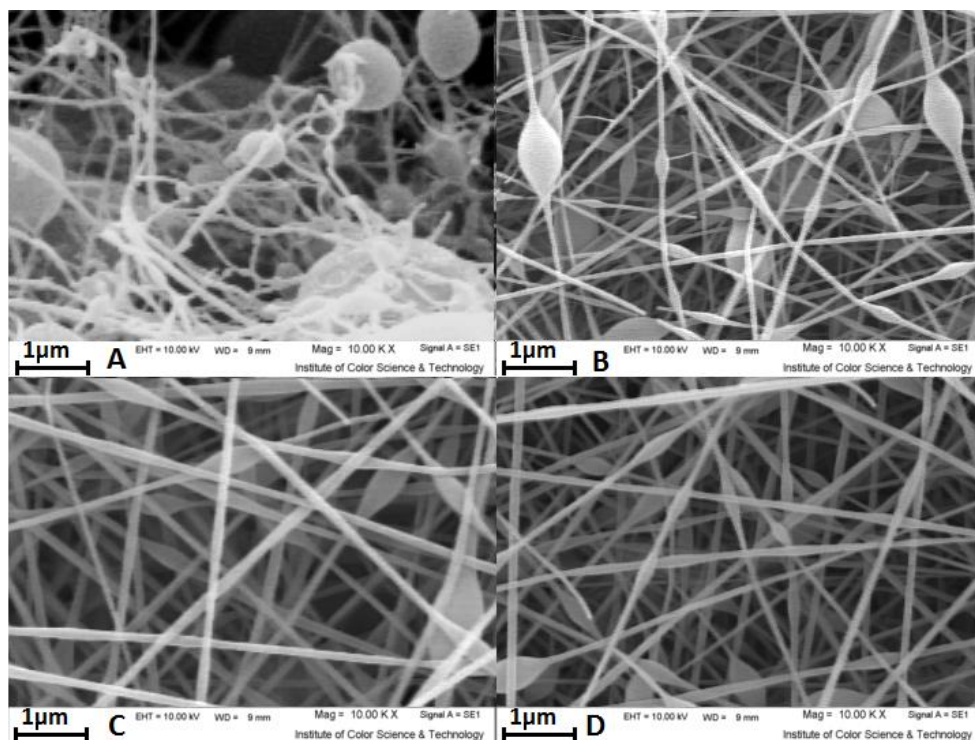

Fig. 3. The SEM images of PDDA/honey nanofibers with the concentration ratio of 50/50%w/w and the flow rate of 0.8mL/h at the voltage of A) 14-17kV, B) 19kV, C) 20kV and D) 22kV

PDDA/honey solutions at the shear rate of 10^0 was 0.791, 22.1, 2.28, 4.17, 5.91, 7.01 and 9.18 *Pa.s.*, respectively. It was clear that solution viscosity increased with raising the honey concentration.

Fig. 3 showed the SEM images of PDDA/ honey nanofibers with the concentration ratio of 50/50%*w/w* at different applied voltages and

the flow rate of 0.8 *mL/h*. From the figure, all the nanofibers presented a beaded structure. Also, the diameter of nanofibers was not uniform. The increase in the high voltage values (18-20 *kV*) caused to increase the charge density in the liquid jet and polymer jet velocity. An increment in the velocity of jet increased the applied elongation
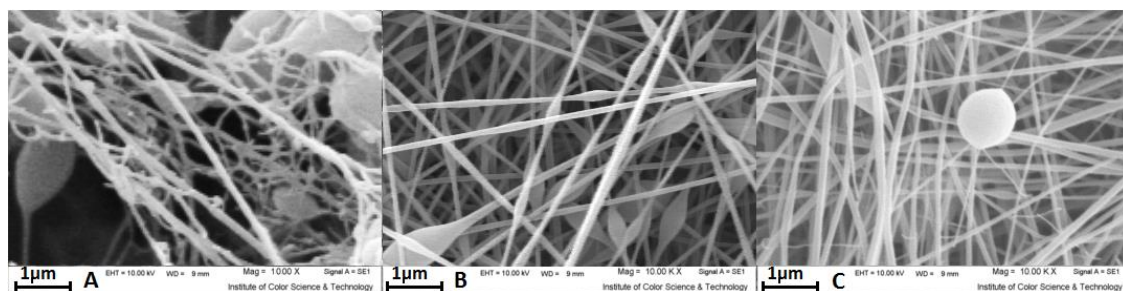
Fig. 4. The SEM images of PDDA/honey nanofibers with the concentration ratio of 50/50%w/w at the voltage of 19kV and the flow rate of A) 0.6mL/h, B) 0.7mL/h, and C) 0.8mL/h

forces resulted to more uniform morphology of nanofibers and decreasing the amount of beads. However, the shape of droplet on the tip of needle was not uniform during the spinning process. Also, receded jets, which were not stable jets, were replaced by cone jets and caused to increase the un-uniformity [39].

At low high voltage values (14-17 kV), the applied electric field was not strong enough to provide a balance between the electrostatic repulsion, the surface tension and viscoelastic force resulted to formation of a beaded structure. In the electrospinning process, providing a balance between the surface tension, electrostatic repulsion, and viscoelastic forces results a uniform morphology of nanofibers [33]. In this study, the effects of viscoelasticity and charge density on fiber morphology were evaluated by varying the concentration ratio of polymer and voltage, respectively. With increasing the high voltage values (18-20 kV), the fibrous structure was obvious and the amount of bead was decreased. However, the dividing of polymer droplet on the tip of needle to small droplets was occurred which can be due to the low viscosity of the spinning solution. An investigation on the average nanofiber diameter revealed that increasing the voltage value from 18 to 19 kV caused to decrease the nanofiber diameter. However, the diameter was increased when the voltage rose to 20 kV (Fig. 3C). Increasing the nanofiber diameter with increasing the high voltage value is reported by researchers [40]. Further increase in the voltage value (22 kV) resulted to raising the amount of bead probably due to the unbalance conditions of electrospinning process.

The effect of flow rate on nanofiber morphology was also investigated at the voltage of 19 kV and the result is shown in the Fig. 4. It was found that the beaded structure was obtained with the flow rate of 0.6 mL/h. Increasing the flow rate to 0.8 mL/h resulted to more uniform morphology with lower amount of bead compared to 0.7 mL/h probably because of the existence of a balance between the amounts of injection and feeding of polymer in the spinning process.

Fig. 5 presented the SEM images of nanofibers produced with the honey concentration of 60%w/w with the flow rate of 0.8 mL/h. It was clear that increasing the honey concentration to 60%w/w was enhanced significantly the uniformity of the produced nanofibers. An increment in the voltage value from 14.5 to 16.5 kV caused to decrease the nanofiber diameter due to the stretching of the polymer droplet along with charge repulsion within the polymer jet [40]. Raising the voltage value (14.5 to 16.5 kV) resulted in enhancing the uniformity of nanofiber diameter because of the stability of the jet due to increased charge density on the surface of jet, the jet velocity and the applied elongation forces [41]. The average diameter of nanofibers obtained at the voltage of 16.5 kV was 94.1nm. The average diameter of PDDA/honey nanofibers was nearly constant in the voltage range of 17-19 kV. Previously, it is reported that for certain polymers, increasing the applied voltage did not effect on the diameter and morphology of nanofibers [42]. The nanofibers with smooth surface, uniform morphology and the average diameter of 91.8 nm were obtained at the high voltage of 19 kV. Further increase in the voltage value changed the morphology of nanofibers from round to ribbon-like shape. Increasing the high voltage caused to apply high electrostatic and elongation forces to the droplet and liquid jet. Hence, the polymeric jet moves faster toward the collector and the solvent may not dry completely before reaching the collector. These reasons led to
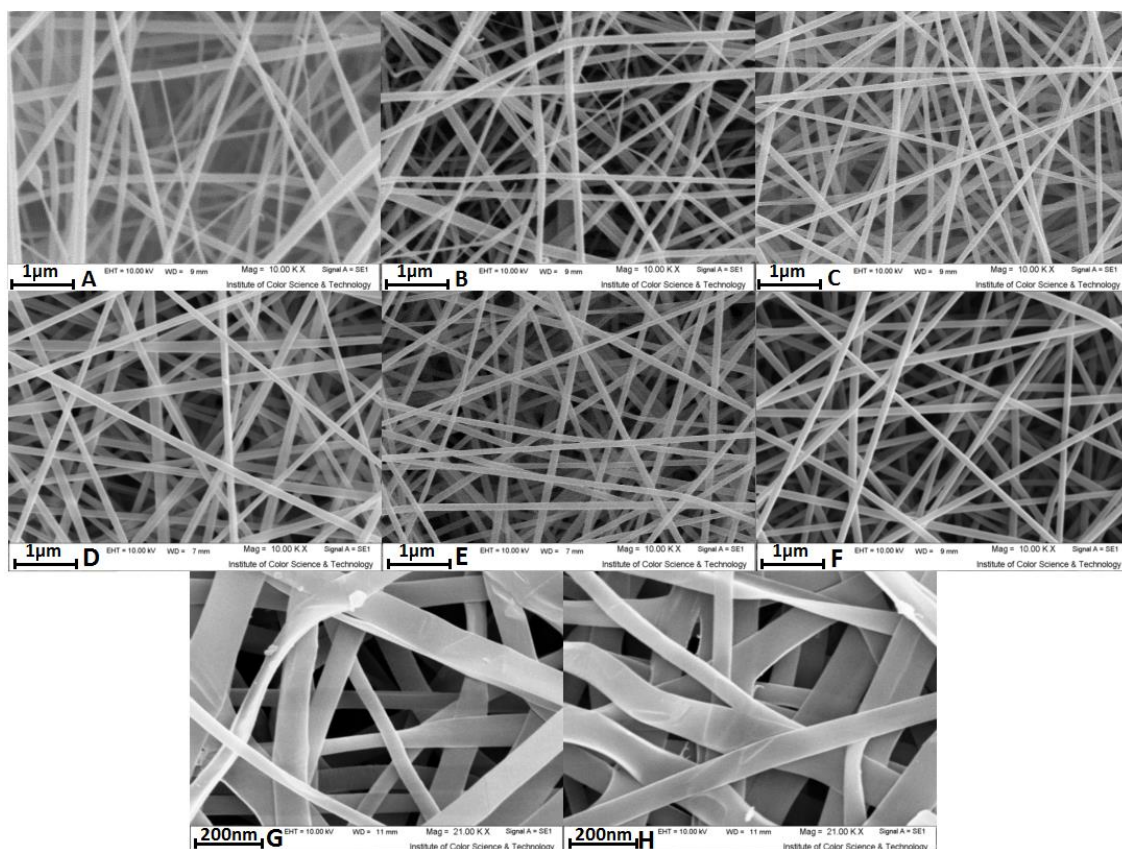
Fig. 5. The SEM images of PDDA/honey nanofibers with the concentration ratio of 40/60%w/w with the flow rate of 0.8mL/h and the voltage of A) 14.5kV, B) 15.5kV, C) 16.5kV, D) 17kV, E) 18kV, F) 19kV, G) 21kV and H) 22kV

the formation of ribbon-like structure. Moreover, the width of nanofibers increased with raising the voltage values.

Fig. 6 showed the distribution of nanofiber diameter with the high voltage range of 14.5-16.5 and 17-19 kV. It was clear that the nanofibers produced with the voltage of 14.5 kV presented a relatively wide distribution with the center of 124 nm compared to the other samples. The diameter distribution became narrow when the applied voltage rose to 16.5 kV. The average diameter of nanofibers produced at the high voltage of 15.5 and 16.5 kV was 108.4 and 94.1 nm, respectively. This can be probably due to the more stable condition of electrospinning process resulted to produce bead-free nanofibers with more uniform diameter. The diameter distribution of nanofibers obtained at the high voltage range of 17-19 kV exhibited a narrow structure with the center of 93.5, 92.7 and 91.8 nm for the voltage of 17, 18 and 19 kV, respectively.

The effect of flow rate on the nanofiber morphology was investigated for the PDDA/honey nanofibers with the honey concentration of 60%w/w at the high voltage of 19 kV and the result is shown in Fig. 7. It was found that the nanofibers were not obtained when the flow rate was lower than 0.35 mL/h. This can be due to insufficient amount of solution in the spinneret. In this case, the Taylor cone at the tip of needle could not be formed. With increasing the flow rate to 0.6 mL/h, uniform nanofibers with round cross section were produced. According to the Fig. 7, the uniform morphology was maintained when the flow rate was increased from 0.6 to 0.8 mL/h. On the other hand, an increment in the flow rate from 0.6 to 0.8 mL/h increased the nanofiber diameter from 79 to 91.8 nm, respectively. Increasing the flow rate to 1 mL/h caused to form the ribbon-like structure because of incomplete evaporation of solvent resulted from high amount of injected polymer [43].

An increment in the content of honey caused to increase the spinning viscosity. At the low viscosity
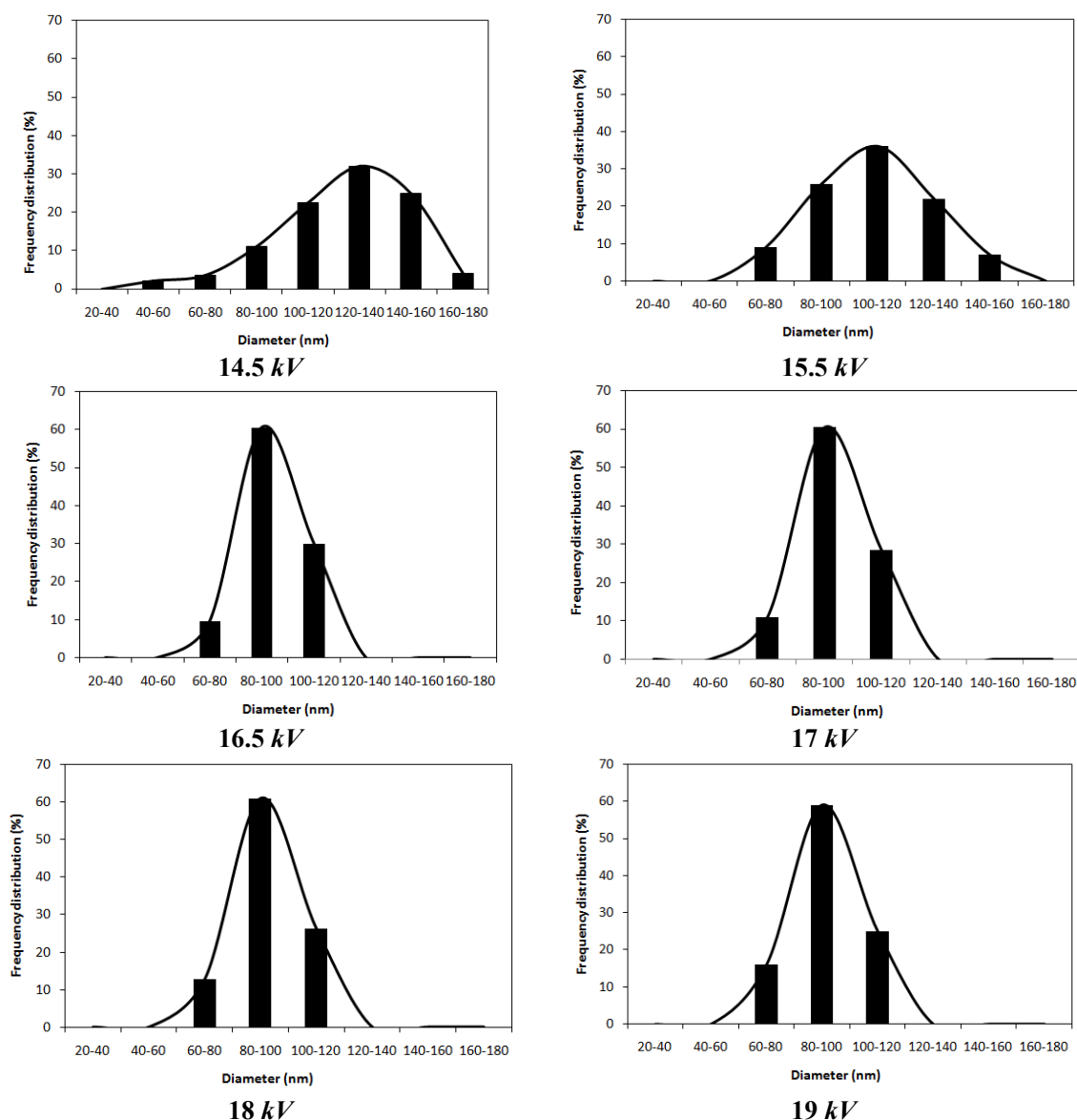
Fig. 6. the distribution of nanofiber diameter with the high voltage range of 14.5-16.5 and 17-19 *kV*.

(PDDA/honey with the concentration ratio of 50/50%*w/w*), the mobility of the PDDA polymer chains was high and the strong instabilities of the jets occurred during the spinning process. These were resulted to formation of beads in the nanofiber morphology. Increasing the viscosity resulted from the increment of honey content in the spinning solution increased the entanglement of polymer chains. Hence, the liquid jet was more stable and fibrous morphology was obvious. Such a result is reported by researchers [42,44]. According to the results of the microscopic analysis, the PDDA/

honey nanofibers with the concentration ratio of 40/60%w/w obtained at the high voltage of 17kV and the flow rate of 0.8mL/h were selected as the optimum and used for crosslinking procedure and further studies. The crosslinking of nanofibers was performed by glutaraldehyde. The SEM images of the crosslinked nanofibers with different crosslinking time are shown in Fig. 8. According to the images, some conglutinations of nanofibers especially at their touching points and some cracks on the nanofiber surface were observed. Increasing the time of crosslinking changed the morphology
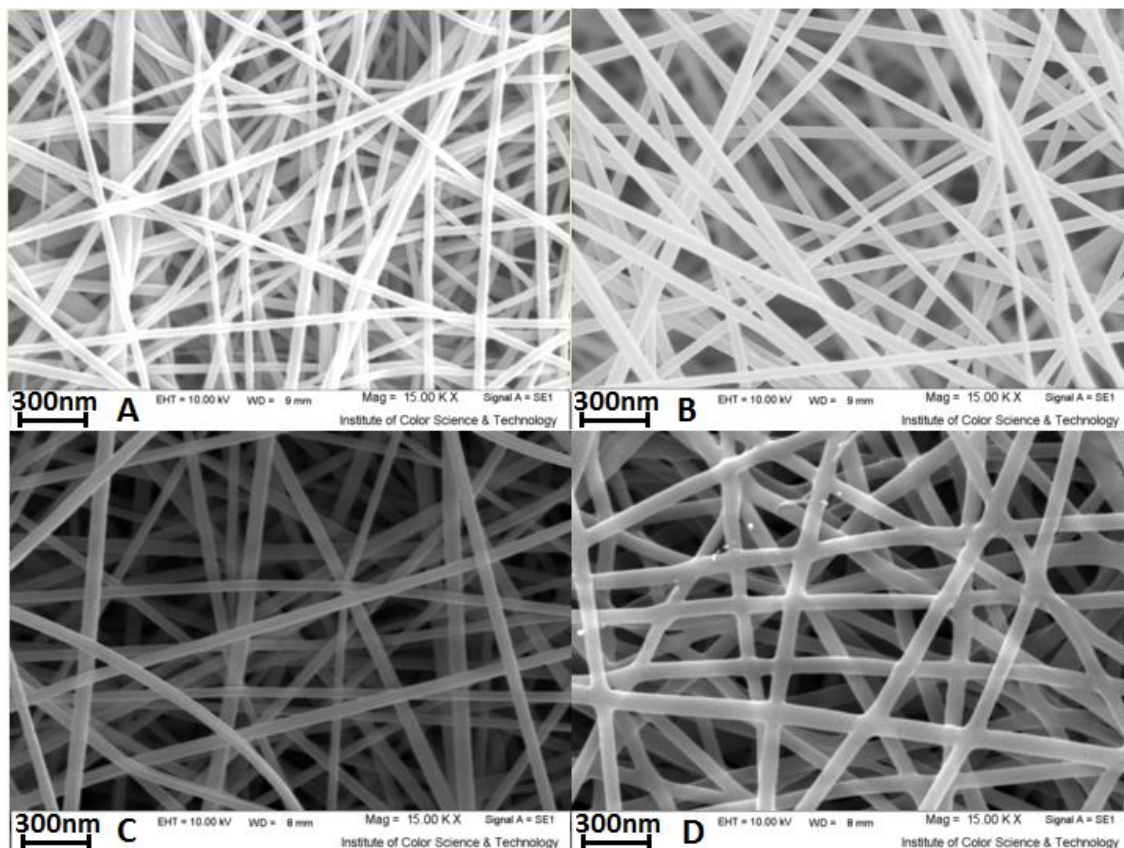
Fig. 7. The SEM images of PDDA/honey nanofibers with the concentration ratio of 40/60%w/w at the voltage of 19kV and the flow rate of A) 0.6mL/h, B) 0.7mL/h, C) 0.8mL/h and D) 1mL/h

from fibrous to film like structure.

The FTIR spectra of PDDA, PDDA/honey (40/60%*w/w*) and crosslinked PDDA/honey samples are shown in Fig. 9. In the PDDA spectrum, the band at 3434 and 1631 cm^{-1} were attributed to the stretching and bending vibrations of absorbed water molecules, respectively. Also, the appeared band at 1205 cm^{-1} was related to the stretching vibration of C-N bond [45]. The peak observed at 1460 $cm^{-1}$is due to CH_2 bending vibration. The bands at 2931 and 2898 cm^{-1} assigned to the methylene C-H asymmetric and symmetric stretching vibrations, respectively. The honey composed of mainly hydrated glucose, fructose and carbohydrates. The skeletal vibrations carbohydrates were appeared in the range of 600-1500 cm^{-1} [30]. Also, the band at 3443 cm^{-1} was related to the stretching vibration of OH groups of carbohydrate. The appeared band at 2994 and 2841 cm^{-1} were assigned to the stretching vibrations of CH bonds. The band at 1513 cm^{-1} is attributed to the vibration of C=C bond in the aromatic ring [46]

of polyphenols in the honey. Amino acids, existed in the honey, generally contain amide groups with several characteristic bands as amide A (about 3500 cm^{-1}), amide B (about 3100 cm^{-1}), amide I (1600–1700 cm^{-1}), amide II (1550 cm^{-1}) and amide III (1300–1350 cm^{-1}) depending on the type and amount of amino acids. The characteristic peaks of PDDA overlapped with the honey characteristic peaks. By comparing the curves B and C, it was found that the intensity of bands at 1059, 2936, 2848 and 1731 cm^{-1} increased which were related to the acetal band [47], resulted from the reaction of glutaraldehyde with the hydroxyl group of honey, the stretching vibrations of CH bonds and the stretching vibration of C=O groups, existing in the glutaraldehyde [34], respectively. Also, the intensity of the band at 3446 was cm^{-1} decreased due to the reaction of crosslinking agent with OH groups of honey. A new absorption peak at 1690 cm^{-1} was related to the imine group [48], resulted from the reaction of glutaraldehyde and amine group of honey contents.
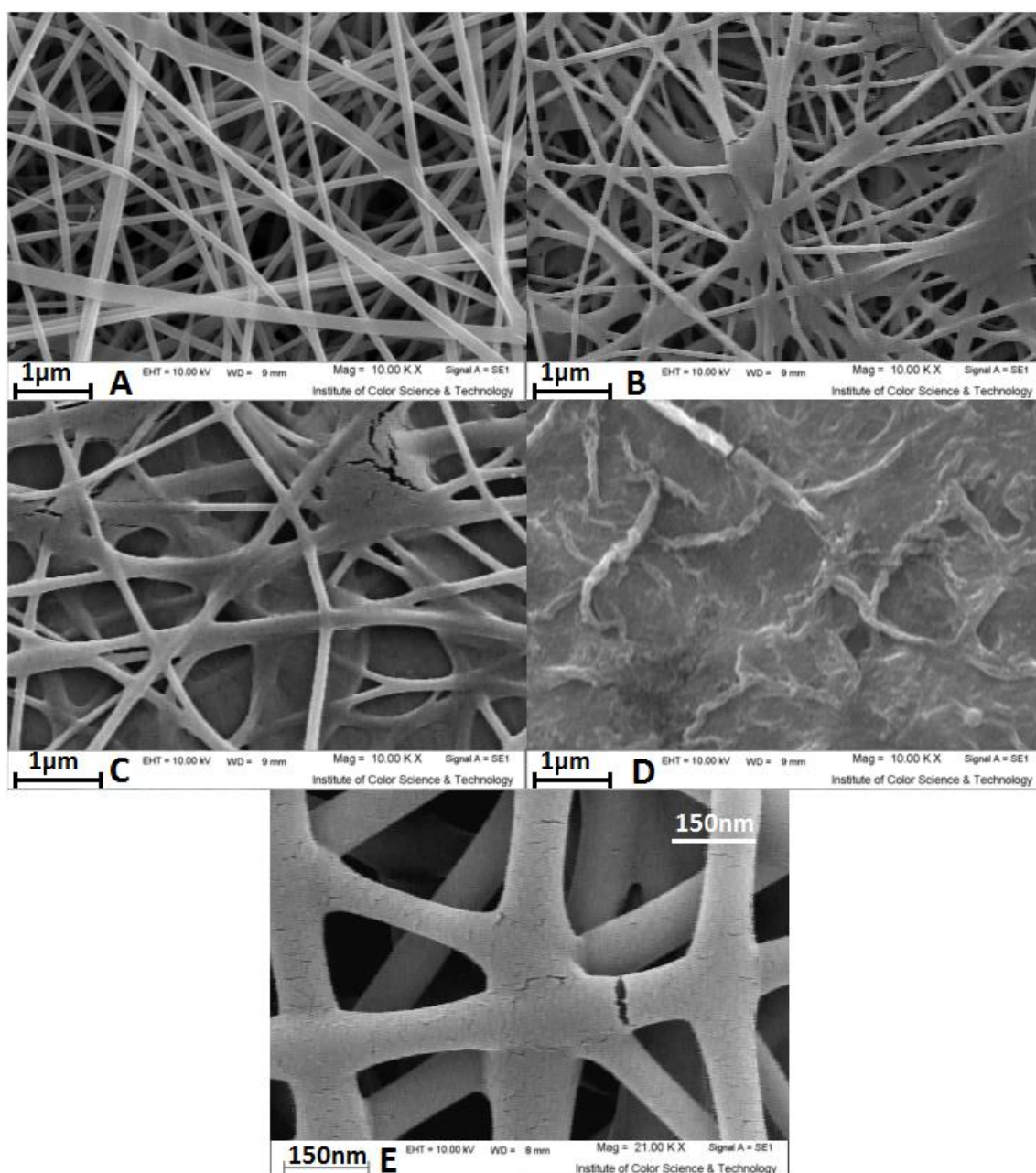
Fig. 8. The SEM images of the crosslinked PDDA/honey nanofibers with the time of: A) 2h, B & E) 3h, C) 4h and D) 5h

The wound moist environment is an ideal growth medium for bacteria. Infection has been identified as a major factor in impaired healing. Wound infections are largely treated with antibiotics in conventional medicine however, it is often inappropriate in cases such as burns and chronic wounds. In this regard, dressing technology is known as alternative options. Among the various materials used in wound dressing, honey containing dressing materials is highly desired due to the ability of control the level of wound hydration and its antimicrobial property [49].

The amount of water uptake of nanofibers was measured as 0.4, 4.9, 3.6 and 0.2 g/g for the crosslinked nanofibers with the crosslinking time of 2, 3, 4 and 5 h. Increasing the time of crosslinking changed the morphology of nanofibers. Also, the crosslinked nanofibers with the time of 4 and 5 h
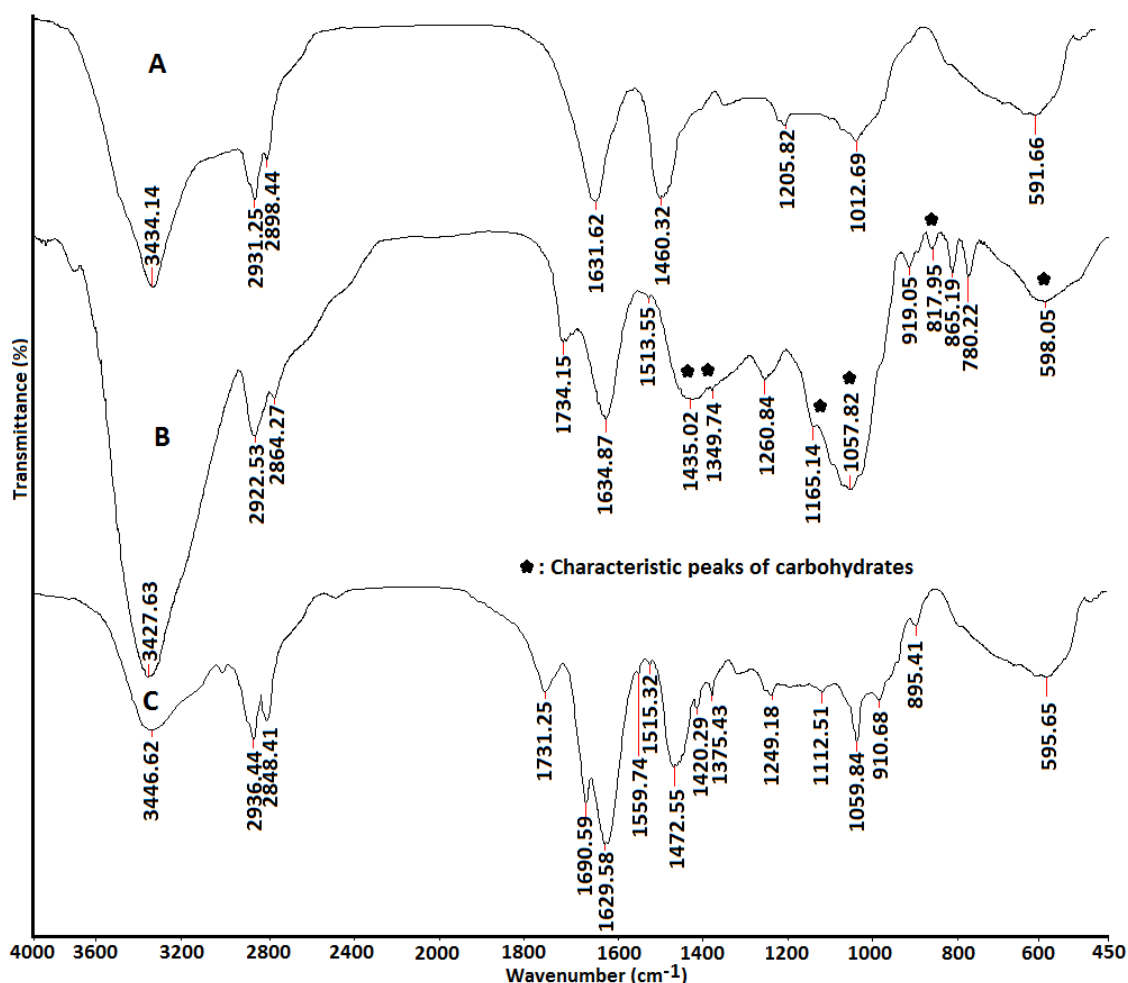
Fig. 9. The FTIR spectra of A) PDDA, B) PDDA/honey (40/60%w/w) and C) crosslinked PDDA/honey (40/60%w/w).

presented a rigid structure with no flexibility which is not favor for wound dressing. Increasing the time of crosslinking caused to change the hydrophilic nature of the nanofiber surface, hindering the penetration of water molecules in to the nanofiber mats. The result of nanofibers solubility revealed that the samples crosslinked with the time of 2 *h* showed a weight loss of 39.3% whereas there was not any weight loss for the other samples. In this regard, the crosslinking time of 3 *h* was selected as optimum.

The antibacterial activity of PDDA and PDDA/honey nanofiber (40/60%*w/w*) samples were studied by using the viable cell-counting method. The effects of nanofibers on the growth of the gram-positive and gram-negative bacteria (S. aureus and E. coli), also antibiotic resistant bacteria (P. aeruginosa) were investigated and the results are

shown in Fig. 10 and 11. Fig. 10 as shown in the plates, the number of bacteria colonies decreased after the addition of honey to the nanofibers. For the PDDA/honey nanofiber sample, of E. coli and S. aureus with initial number concentration of 5×10^5 CFU/mL were completely eradicated whereas there were some bacterial colonies for the PDDA sample. Also, the antibacterial efficiency of PDDA sample for E. coli was slightly higher than S. aureus. The antibacterial efficiency of PDDA sample was 77.8 and 81.2% for S. aureus and E. coli, respectively. Additionally, PDDA/honey nanofiber (40/60%*w/w*) antibacterial activity against P. aeruginosa was studied using same study condition of S. aureus and E. coli, results indicated antibacterial efficiency of antibiotic free PDDA/honey nanofiber was suitable. PDDA/honey nanofiber (40/60%*w/w*) determined 98.89% antibacterial efficiency for
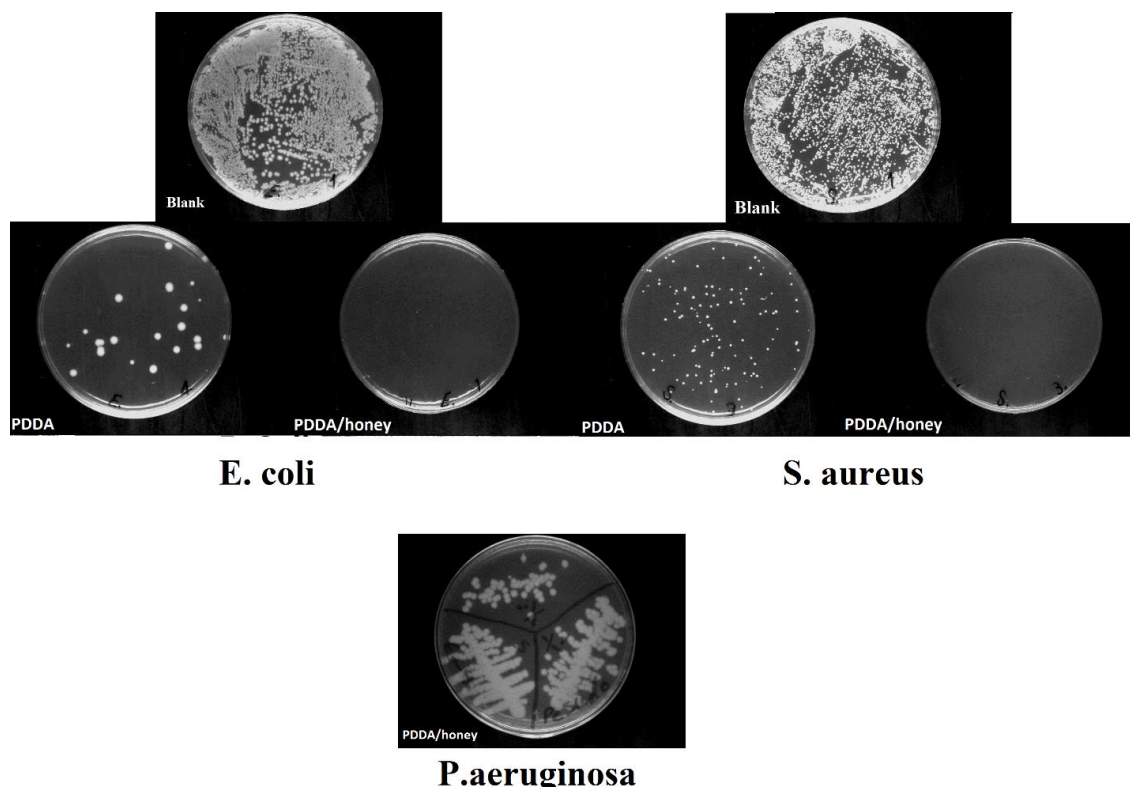
E. coli **S. aureus**

P.aeruginosa

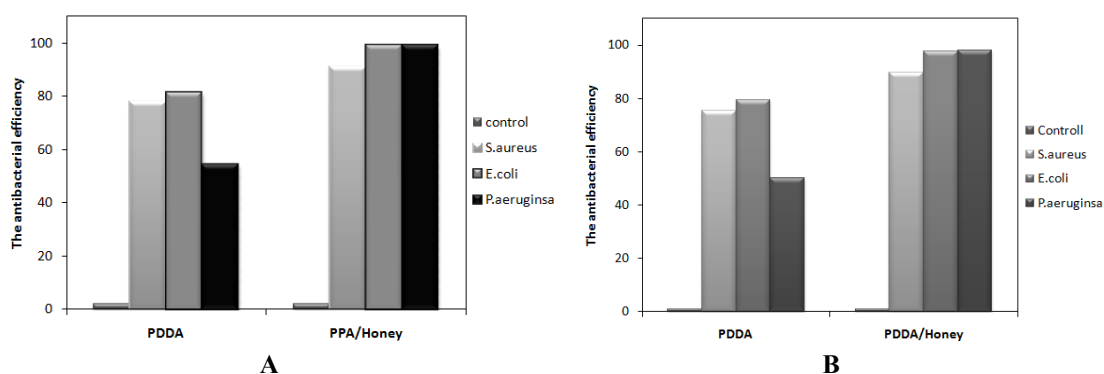Fig. 10. The antibacterial activity of PDDA/honey nanofibers against E. coli, S. aureus and P. aeruginosa.

Fig. 11. The antibacterial activity of PDDA/honey nanofibers on E. coli, S. aureus and P. aeruginosa (A) before dilution and (B) after dilution.

P. aeruginosa as important medically the genus Pseudomonas. The antibacterial activity of PDDA as a polycation polymer is related to permanently charge quaternary ammonium groups in its cyclic unities which interact with the negatively charged surfaces of bacteria, resulting in loss of membrane permeability, cell leakage, and finally cell death [24]. The antibacterial property of honey was related to the H_2O_2 and antioxidant polyphenols existing among its compounds. Polyphenols in the presence of transition metal ions play a powerful pro-oxidants role, stimulating the generation of hydroxyl radicals from H_2O_2 via the Fenton reaction [50]. The antibacterial efficiency of PDDA/honey antibiotic free nanofiber was 99.9 % for S. aureus and E. coli. The results showed synergistic

86

antibacterial effect of the PDDA/honey blend composite, compared to honey or PDDA only. Moreover, antibacterial PDDA/honey nanofiber dilution did not show a significant effect on the antibacterial response (Fig. 11).

CONCLUSION

In this research, the ability of producing the PDDA nanofibers was investigated for first time. The result showed that the PDDA nanofibers with the beaded morphology can be obtained with high molecular weight of polymer and producing the PDDA nanofiber with low molecular weight of polymer is impossible. However, the reproducibility of nanofibers was not feasible at the same condition. In order to obtain a uniform morphology, different concentrations of honey were added to the spinning solution. The addition of honey increased the solution viscosity and entanglement of polymer chains. The bead-free nanofibers with uniform diameter were obtained with concentration ratio of 40/60 (PDDA/honey). Increasing the high voltage values caused to decrease the nanofibers average diameter. However, the average diameter of nanofibers was nearly constant when the high voltage ranged from 17 to 19 kV. Increasing the flow rate of spinning solution increased the average diameter of nanofibers. An increment of flow rate to 1 mL/h and voltage value to 21 kV resulted in formation of ribbon-like structure due to incomplete evaporation of solvent and high applied electrostatic and elongation forces to the droplet and liquid jet. The use of the same concentration of PDDA and honey resulted to formation of beaded structure. The density of beads was reduced with varying the electrospinning parameters (high voltage and flow rate values). However, nanofibers with uniform diameter and bead-free morphology were not obtained due to the low viscosity of spinning solution. Crosslinked nanofibers showed a high water absorption capacity and antibacterial property. Moreover, PDDA/honey antibiotic free nanofibers showed great antibacterial activity (99.9 %) against S. aureus and E. coli and suitable activity (98.9) against pathogenic bacteria (P. aeruginosa). Finally, PDDA/honey antibiotic free nanofibers with suitable antibacterial activity can be used as a nanoantibiotic against gram-positive and gram-negative bacteria, such as pathogenic P. aeruginosa as medically the genus Pseudomonas. As well as, it can be suggested that the prepared novel antibiotic free nanofibers can be a good candidate for wound dressing.

CONFLICT OF INTEREST

The authors declare that there are no conflicts of interest.

REFERENCES

1. Meeker DG, Jenkins SV, Miller EK, Beenken KE, Loughran AJ, Powless A, et al. Synergistic Photothermal and Antibiotic Killing of Biofilm-Associated Staphylococcus aureus Using Targeted Antibiotic-Loaded Gold Nanoconstructs. ACS Infectious Diseases. 2016;2(4):241-50.
2. Bassetti M, Merelli M, Temperoni C, Astilean A. New antibiotics for bad bugs: where are we? Annals of Clinical Microbiology and Antimicrobials. 2013;12(1):22.
3. Gellatly SL, Hancock REW. Pseudomonas aeruginosa: new insights into pathogenesis and host defenses. Pathogens and Disease. 2013;67(3):159-73.
4. Spiers AJ, Buckling A, Rainey PB. The causes of Pseudomonas diversity. Microbiology. 2000;146(10):2345-50.
5. Silby MW, Winstanley C, Godfrey SAC, Levy SB, Jackson RW. Pseudomonas genomes: diverse and adaptable. FEMS Microbiology Reviews. 2011;35(4):652-80.
6. Juayang A, Lim J, Bonifacio A, Lambot A, Millan S, Sevilla V, et al. Five-Year Antimicrobial Susceptibility of Pseudomonas aeruginosa from a Local Tertiary Hospital in Bacolod City, Philippines. Tropical Medicine and Infectious Disease. 2017;2(3):28.
7. Coggan KA, Wolfgang MC. Global regulatory pathways and cross-talk control Pseudomonas aeruginosa environmental lifestyle and virulence phenotype. Curr Issues Mol Biol. 2012, 14(2):47-70.
8. Aloush V, Navon-Venezia S, Seigman-Igra Y, Cabili S, Carmeli Y. Multidrug-Resistant Pseudomonas aeruginosa: Risk Factors and Clinical Impact. Antimicrobial Agents and Chemotherapy. 2005;50(1):43-8.
9. P A Lambert. Mechanisms of antibiotic resistance in Pseudomonas aeruginosa. J R Soc Med 2002, 95 (Suppl. 41), 22-26.
10. Derbali RM, Aoun V, Moussa G, Frei G, Tehrani SF, Del'Orto JC, et al. Tailored Nanocarriers for the Pulmonary Delivery of Levofloxacin against Pseudomonas aeruginosa: A Comparative Study. Molecular Pharmaceutics. 2019;16(5):1906-16.
11. Wang L, Hu C, Shao L. The antimicrobial activity of nanoparticles: present situation and prospects for the future. International Journal of Nanomedicine. 2017;Volume 12:1227-49.
12. Chao Song, Xiangting Dong----Hu, J.; Chen, M.; Fang, X.; Wu, L. Preparation and Characterization of Tetracomponent ZnO/SiO2/SnO2/TiO2 Composite Nanofibers by Electrospinning, Fabrication and Application of Inorganic Hollow Spheres. Chem. Soc. Rev. 2011, 40, 5472–5491
13. An K, Hyeon T. Synthesis and biomedical applications of hollow nanostructures. Nano Today. 2009;4(4):359-73.
14. Jin R, Yang Y, Xing Y, Chen L, Song S, Jin R. Facile Synthesis and Properties of Hierarchical Double-Walled Copper Silicate Hollow Nanofibers Assembled by Nanotubes. ACS Nano. 2014;8(4):3664-70.
15. Zhang Q, Liu J, Wang X, Li M, Yang J. Controlling internal nanostructures of porous microspheres prepared via electrospraying. Colloid and Polymer Science. 2010;288(14-15):1385-91.

16. Sung-Seen Choi, Seung Goo Lee, Seung Soon Im, Seong Hun Kim, Yong L. Joo, Silica nanofibers from electrospinning/sol-gel process, Journal of Materials Science Letters, 22, 2003, 891-893.

17. Dan Li and Younan Xia, Fabrication of Composite and Ceramic Hollow Nanofibers by Electrospinning, 4, 2004, 933-938.

18. Wu Y-n, Li F, Wu Y, Jia W, Hannam P, Qiao J, et al. Formation of silica nanofibers with hierarchical structure via electrospinning. Colloid and Polymer Science. 2011;289(11):1253-60.

19. Dautzenberg H, Görnitz E, Jaeger W. Synthesis and characterization of poly(diallyldimethylammonium chloride) in a broad range of molecular weight. Macromolecular Chemistry and Physics. 1998;199(8):1561-71.

20. Xu Z, Gao N, Dong S. Preparation and layer-by-layer self-assembly of positively charged multiwall carbon nanotubes. Talanta. 2006;68(3):753-8.

21. Liu K, Zhang J, Yang G, Wang C, Zhu J-J. Direct electrochemistry and electrocatalysis of hemoglobin based on poly(diallyldimethylammonium chloride) functionalized graphene sheets/room temperature ionic liquid composite film. Electrochemistry Communications. 2010;12(3):402-5.

22. Nizri G, Lagerge S, Kamyshny A, Major DT, Magdassi S. Polymer–surfactant interactions: Binding mechanism of sodium dodecyl sulfate to poly(diallyldimethylammonium chloride). Journal of Colloid and Interface Science. 2008;320(1):74-81.

23. Zhang L, Chen H, Sun J, Shen J. Layer-by-Layer Deposition of Poly(diallyldimethylammonium chloride) and Sodium Silicate Multilayers on Silica-Sphere-Coated Substrate—Facile Method to Prepare a Superhydrophobic Surface. Chemistry of Materials. 2007;19(4):948-53.

24. Lu J, Wang X, Xiao C. Preparation and characterization of konjac glucomannan/poly(diallydimethylammonium chloride) antibacterial blend films. Carbohydrate Polymers. 2008;73(3):427-37.

25. Melo LcD, Mamizuka EM, Carmona-Ribeiro AM. Antimicrobial Particles from Cationic Lipid and Polyelectrolytes. Langmuir. 2010;26(14):12300-6.

26. Sanches LM, Petri DFS, de Melo Carrasco LD, Carmona-Ribeiro AM. The antimicrobial activity of free and immobilized poly (diallyldimethylammonium) chloride in nanoparticles of poly (methylmethacrylate). nano Online: De Gruyter; 2016.

27. Vieira DB, Carmona-Ribeiro AM. Cationic nanoparticles for delivery of amphotericin B: preparation, characterization and activity in vitro. Journal of Nanobiotechnology. 2008;6(1):6.

28. Ozmen N, Alkın E. The antimicrobial features of honey and the effects on human health. Uludag Bee J. 2006;1:155–160.

29. Maleki H, Gharehaghaji AA, Dijkstra PJ. A novel honey-based nanofibrous scaffold for wound dressing application. Journal of Applied Polymer Science. 2012;127(5):4086-92.

30. Arslan A, Şimşek M, Aldemir SD, Kazaroğlu NM, Gümüşderelioğlu M. Honey-based PET or PET/chitosan fibrous wound dressings: effect of honey on electrospinning process. Journal of Biomaterials Science, Polymer Edition. 2014;25(10):999-1012.

31. Matabola KP, Moutloali RM. The influence of electrospinning parameters on the morphology and diameter of poly(vinyledene fluoride) nanofibers- effect of sodium chloride. Journal of Materials Science. 2013;48(16):5475-82.

32. Zhang M, Cheng Z, Zhao T, Liu M, Hu M, Li J. Synthesis, Characterization, and Swelling Behaviors of Salt-Sensitive Maize Bran–Poly(acrylic acid) Superabsorbent Hydrogel. Journal of Agricultural and Food Chemistry. 2014;62(35):8867-74.

33. Haider A, Haider S, Kang I-K. A comprehensive review summarizing the effect of electrospinning parameters and potential applications of nanofibers in biomedical and biotechnology. Arabian Journal of Chemistry. 2018;11(8):1165-88.

34. Almasian A, Mahmoodi NM, Olya ME. Tectomer grafted nanofiber: Synthesis, characterization and dye removal ability from multicomponent system. Journal of Industrial and Engineering Chemistry. 2015;32:85-98.

35. Son WK, Youk JH, Lee TS, Park WH. The effects of solution properties and polyelectrolyte on electrospinning of ultrafine poly(ethylene oxide) fibers. Polymer. 2004;45(9):2959-66.

36. Witczak M, Juszczak L, Gałkowska D. Non-Newtonian behaviour of heather honey. Journal of Food Engineering. 2011;104(4):532-7.

37. Gómez-Díaz D, Navaza JM, Quintáns-Riveiro LC. Rheological behaviour of Galician honeys. European Food Research and Technology. 2005;222(3-4):439-42.

38. Saxena S, Panicker L, Gautam S. Rheology of Indian Honey: Effect of Temperature and Gamma Radiation. International Journal of Food Science. 2014;2014:1-6.

39. Zargham S, Bazgir S, Tavakoli A, Rashidi AS, Damerchely R. The Effect of Flow Rate on Morphology and Deposition Area of Electrospun Nylon 6 Nanofiber. Journal of Engineered Fibers and Fabrics. 2012;7(4):155892501200700.

40. Sill TJ, von Recum HA. Electrospinning: Applications in drug delivery and tissue engineering. Biomaterials. 2008;29(13):1989-2006.

41. Ding W, Wei S, Zhu J, Chen X, Rutman D, Guo Z. Manipulated Electrospun PVA Nanofibers with Inexpensive Salts. Macromolecular Materials and Engineering. 2010;295(10):958-65.

42. Jing H, Du X, Jiang Y. Control of diameter and morphology of poly(vinylidene fluoride) nanofibers fabricated by electrospinning. 2009 International Conference on Optical Instruments and Technology: Advanced Sensor Technologies and Applications; 2009/11/04: SPIE; 2009.

43. Meng L, Klinkajon W, K-hasuwan P-r, Harkin S, Supaphol P, Wnek GE. Electrospun crosslinked poly(acrylic acid) fiber constructs: towards a synthetic model of the cortical layer of nerve. Polymer International. 2014;64(1):42-8.

44. Jacobs V, Anandjiwala RD, Maaza M. The influence of electrospinning parameters on the structural morphology and diameter of electrospun nanofibers. Journal of Applied Polymer Science. 2010;115(5):3130-6.

45. Zia KM, Anjum S, Zuber M, Mujahid M, Jamil T. Synthesis and molecular characterization of chitosan based polyurethane elastomers using aromatic diisocyanate. International Journal of Biological Macromolecules. 2014;66:26-32.

46. Almasian A, Jalali ML, Fard GC, Maleknia L. Surfactant grafted PDA-PAN nanofiber: Optimization of synthesis, characterization and oil absorption property. Chemical

Engineering Journal. 2017;326:1232-41.

47. Mahmoodi NM, Mokhtari-Shourijeh Z. Preparation of PVA-chitosan blend nanofiber and its dye removal ability from colored wastewater. Fibers and Polymers. 2015;16(9):1861-9.

48. Mahmoodi NM, Mokhtari-Shourijeh Z. Modified poly(vinyl alcohol)-triethylenetetramine nanofiber by glutaraldehyde: preparation and dye removal ability from wastewater. Desalination and Water Treatment. 2015;57(42):20076-83.

49. Mohamed H, Salma MA, Al Ienjawi B, Abdi S, Gouda Z, Barakat N, Elmahdi H, Abraham S, Hamza AH, Al Khozaei D, Al Majid S, Al Majid H, Abdini J, Al Jaber M, Al Masseh F, Al Ali AA. The efficacy and safety of natural honey on the healing of foot ulcers: a case series. Wounds. 2015;27:103-14.

50. Brudzynski K, Abubaker K, Miotto D. Unraveling a mechanism of honey antibacterial action: Polyphenol/ H2O2-induced oxidative effect on bacterial cell growth and on DNA degradation. Food Chemistry. 2012;133(2):329-36.